Metal–Organic Frameworks

DOI: 10.1002/ange.201105966

Enhanced Binding Affinity, Remarkable Selectivity, and High Capacity of CO_2 by Dual Functionalization of a *rht*-Type Metal–Organic Framework**

Baiyan Li, Zhijuan Zhang, Yi Li, Kexin Yao, Yihan Zhu, Zhiyong Deng, Fen Yang, Xiaojing Zhou, Guanghua Li, Haohan Wu, Nour Nijem, Yves J. Chabal, Zhiping Lai, Yu Han, Zhan Shi, Shouhua Feng, and Jing Li**

As a new family of adsorbent materials, porous metal–organic frameworks (MOFs) have attracted enormous attention over the past decade.[1] Having a large surface area,[2] tunable pore size and shape,[3] adjustable composition and functionalizable pore surface,[4] MOFs show unique advantages and promises for potential applications in adsorption-based storage and separation technologies for small gas molecules such as H_2, CO_2, and CH_4.[1b,d,5]

CO_2 capture from flue gases is of particular importance in reducing greenhouse gas emissions and in preserving environmental health. A flue gas mixture is composed of nitrogen, carbon dioxide, water vapor, oxygen, and other minor components such as carbon monoxide, nitrogen oxides, and sulfur oxides.[1b,6] Separation of low-concentration CO_2 (about 10–15%) from nitrogen-rich streams remains a challenging task at the present time. Adsorption-based CO_2 capture and separation is considered an effective way and may have a real potential if adsorbents with both high CO_2 selectivity and capacity near room temperature (up to 50 °C) and in the low-pressure range can be developed.[7] Recent studies have revealed a number of MOFs that show a high performance in capturing and separating CO_2 from N_2 and other small gases under conditions mimicking power plant flue gas mixtures.[8]

To increase the gas uptake capacity, current efforts are devoted to enhancing the gas-binding affinity in MOFs.[5] Strategies reported include framework interpenetration,[9] ligand functionalization,[1e,4b,10] construction of size/shape specific pores and polar pore walls,[3,4b,11] and in particular, incorporation of open metal sites (OMSs).[1d,8a,12] The *rht*-type MOFs built on supramolecular building blocks (SBBs)[13] serve as excellent examples. The SBBs in *rht*-MOFs are constructed by linking three isophthalate moieties of dendritic hexacarboxylate ligands to 24 "square paddlewheel" $M_2(COO)_4$ units, forming a cuboctahedron cluster.[12f,g,13a,14] Notably, all *rht*-MOFs possess a high concentration of OMSs and all are highly porous with large surface area and pore volume. A number of recent studies clearly show that their CO_2 uptake capacity is among the highest reported to date.[12f,g,14,15]

However, with the isosteric heats of CO_2 adsorption in the range of 21–26 kJ mol^{-1} (Table 1), the CO_2 binding affinity in these OMS-rich structures is only moderate and not sufficiently high for optimum performance. To further enhance CO_2–MOF interactions, we have developed a strategy to incorporate two different types of functionality simultaneously in the MOF framework. In addition to a OMS-rich SBB, a ligand containing a high density of Lewis basic sites (LBSs) is synthesized and employed in the construction of new *rht*-type MOFs, taking into consideration the fact that LBS interacts strongly with CO_2.[4b,11b,12g,16]

$[Cu_3(TDPAT)(H_2O)_3]\cdot 10\,H_2O\cdot 5\,DMA$ (Cu-TDPAT) (**1**) is synthesized by using 2,4,6-tris(3,5-dicarboxylphenylamino)-1,3,5-triazine (H_6TDPAT), a LBS-rich hexacarboxylate ligand (see Scheme S1 in the Supporting Information). Based on our molecular simulation calculations, H_6TDPAT is most likely the shortest member of hexacarboxylic acids that can generate the same type of *rht*-type structures. As shown in Scheme S2 in the Supporting Information, any other shorter hexacarboxylates such as 3,3′,3″,5,5′,5″-benzene-1,3,5-triyl-hexabenzoic acid (H_6BHB) will lead to an inter-SBB distance (4.9 Å) that is too short to accommodate two terminal water molecules. Thus, Cu-TDPAT may well be the smallest member of *rht*-nets and represents the first example of MOFs that possesses a high density of both OMSs (1.76 nm^3)

[*] Dr. B. Li, Dr. Y. Li, F. Yang, X. Zhou, Dr. G. Li, Prof. Dr. Z. Shi, Prof. Dr. S. Feng
State Key Laboratory of Inorganic Synthesis and Preparative Chemistry, College of Chemistry
Jilin University, Changchun 130012 (P.R. China)
E-mail: zshi@mail.jlu.edu.cn

Z. Zhang, H. Wu, Prof. Dr. J. Li
Department of Chemistry and Chemical Biology
Rutgers University
610 Taylor Road, Piscataway, NJ 08854 (USA)
E-mail: jingli@rutgers.edu

K. Yao, Y. Zhu, Z. Deng, Prof. Dr. Z. Lai, Prof. Dr. Y. Han
Advanced Membranes and Porous Materials Center
King Abdullah University of Science and Technology (Saudi Arabia)

N. Nijem, Prof. Dr. Y. J. Chabal
Department of Materials Science and Engineering
University of Texas at Dallas, Richardson, TX 75080 (USA)

[**] This work was supported by the Foundation of the National Natural Science Foundation of China (grant numbers 20971054 and 90922034) and the Key Project of the Chinese Ministry of Education. The RU and UTD teams would like to acknowledge support from DOE (grant number DE-FG02-08ER46491). We thank Prof. Xianhe Bu and Dr. Ze Chang (Nankai University, China) and Dr. Ruiping Chen (Fujian Institute of Research on the Structure of Matter, Chinese Academy of Sciences) for part of the gas adsorption measurements.

Supporting information for this article is available on the WWW under http://dx.doi.org/10.1002/anie.201105966.

Table 1: Ligand and polyhedron sizes, porosities, density, and isosteric heats of Cu-TDPAT, Cu-TPBTM, NOTT-112, NU-100, and the isoreticular PCN-6X Series. All data except Cu-TDPAT are taken from Refs. [12f], [12g], [14e], and [15].

	Cu-TDPAT	Cu-TPBTM	PCN-61	NOTT-112	PCN-66	PCN-68	NU-100
L [Å][a]	5.0	6.5	6.9	8.6	9.7	11.2	13.71
cub-O_h size [Å]	12	12	12	12	12	12	12
T-T_d size [Å]	9.1	11.6	11.8	13.1	12	14.8	17
T-O_h size [Å]	17.2	18.7	18.8	21.1	20.6	23.2	29.2
BET SA [$m^2 g^{-1}$]	1938	3160	3000	3800	4000	5109	6605
Pore volume [$cm^3 g^{-1}$][b]	0.93	1.27	1.36	1.62	1.63	2.13	2.82
Density [$g cm^{-3}$]	0.782	0.627	0.56	0.503	0.45	0.38	0.273
OMS Density (per nm^3)	1.76	1.27	1.22	0.92	0.81	0.70	0.45
H_2 uptake [wt%][c]	2.65	–	2.25	2.3	1.79	1.87	2.2
$Q_{st}(H_2)$ [$kJ mol^{-1}$][d]	8.29	–	6.36	5.64	6.22	6.09	6.1
CO_2 uptake [wt%][e]	6.2	2.8	1.6	–	0.88	0.44	1.6
$Q_{st}(CO_2)$ [$kJ mol^{-1}$][f]	42.2	26.3	21.0	–	26.2	21.2	–

[a] L is defined as the distance (Å) between the center of the ligand and the center of a terminal benzene ring (see Scheme S1 in the Supporting Information). [b] Pore volumes were calculated from N_2 isotherms. [c] 77 K, 1 atm. [d] Q_{st} of H_2 is defined as the isosteric heat of H_2 adsorption and calculated at zero coverage. [e] 298 K, 0.1 atm. [f] Q_{st} of CO_2 is the isosteric heat of CO_2 adsorption and calculated at zero coverage.

and LBSs (3.52 nm^3). In fact, it has the highest OMS density among all known *rht*-MOFs of the same type (Table 1). Gas adsorption studies show that Cu-TDPAT has a significantly improved CO_2 affinity, as well as the highest CO_2 uptake capacity and selectivity under conditions that mimic flue gas mixtures over all other members of the series.

The three isophthalate moieties in TDPAT are linked through copper paddlewheel units to form cuboctahedral SBBs, which are covalently bonded through the isophthalate moieties (at position-1) to yield a (3,24)-connected *rht*-type network of **1** (Figure 1 and Figure S1 in the Supporting Information). Similar to other reported (3,24)-connected nets, there are three types of cages in **1**, namely, cuboctahedron (cub-O_h), truncated tetrahedron (T-T_d), and truncated octahedron (T-O_h; see Figure S2 in the Supporting Information). The inner spheres of these three cages are smaller than those of all other *rht*-type structures, with 1.2, 0.91, and 1.72 nm in diameter, respectively, as H_6TDPAT is the smallest ligand among all hexacarboxylic acids (Table 1).

Compound **1** is highly porous with exceptional water and thermal stability. The total accessible volume after removal of the guest and coordinated solvent molecules is 70.2% using the PLATON/VOID routine,[17] and the calculated density of the desolvated framework is 0.782 $g cm^{-3}$. Thermogravimetric (TG) and powder X-ray diffraction (PXRD) analysis at various temperatures show that the framework is stable up to 285 °C (see Figures S3 and S4 in the Supporting Information). The water/moisture stability was tested in boiling water (1 day) and in air (30 days). The framework remained intact as clearly indicated by the PXRD patterns of the samples taken after these tests (see Figure S5 in the Supporting Information).

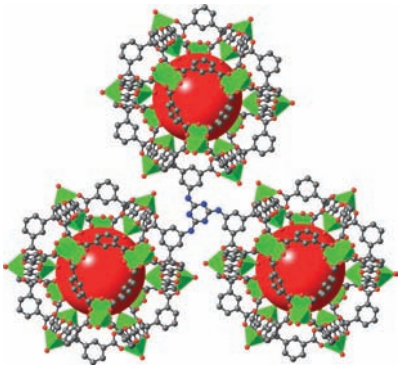

Figure 1. Structure of **1**. A portion of the (3,24)-connected *rht*-net built on the shortest linker TDPAT is shown.

Permanent porosity of activated Cu-TDPAT was confirmed by N_2 adsorption–desorption isotherms at 77 K which show a reversible type-I isotherm (see Figure S6 in the Supporting Information). The Langmuir and BET surface area calculated based on data at the low-pressure region ($P/P_0 = 0.05$–0.2)[18] are 2608 and 1938 $m^2 g^{-1}$, respectively. The total pore volume calculated from the N_2 isotherms is 0.93 $cm^3 g^{-1}$, in good agreement with the value obtained from single-crystal data.

The CO_2 low-pressure adsorption–desorption isotherms were measured at 273, 288, and 298 K (0–1 atm). Compound **1** has a very high CO_2 adsorption capacity. At 298 K, the uptake amount is 132 $cm^3 g^{-1}$ (STP = standard temperature and pressure; 25.8 wt%, 103 *v*/*v*) and 31.3 $cm^3 g^{-1}$ (STP; 6.2 wt%, 24.5 *v*/*v*) at 1.0 and 0.1 atm, respectively. At 273 K, they are 227 $cm^3 g^{-1}$ (STP; 44.5 wt%, 177 *v*/*v*) and 52.8 $cm^3 g^{-1}$ (STP; 10.4 wt%, 41.3 *v*/*v*) at 1.0 and 0.1 atm, respectively (see Table 1, Figure 2 and Figure S7 in the Supporting Information). These values are substantially higher than all previously reported *rht*-type structures (Table 1), and significantly larger than that of the best performing zeolitic imidazolate frameworks (ZIFs), namely ZIF-78 (60.2 *v*/*v*, at 298 K and 1 atm),[4b] and that of zeolite 13X (20.7 wt%, at 298 K and 1 atm),[19] one of the best sorbents for CO_2 separation.

To evaluate the extent of CO_2–MOF interactions, isosteric heats (Q_{st}) of CO_2 adsorption were calculated by the virial[20] method using experimental isotherm data at three temperatures. The Q_{st} values (based on the Clausius–Clapeyron equation) were also obtained directly from experimental data at low loadings by interpolation (AS1Win 2.01).[8c] No fitting was involved in the latter case. The data plotted in Figure S8 in the Supporting Information show excellent agreement by the two methods. Compound **1** shows a very high adsorption enthalpy (42.2 $kJ mol^{-1}$ at zero loading), indicative of strong adsorbate–adsorbent interactions. The Q_{st} values over the entire CO_2 loading range are appreciably higher compared with all other *rht*-type structures reported thus far, following the same trend as the uptake amounts at low pressure. As all *rht*-type MOFs contain a high density of OMSs, this unusually

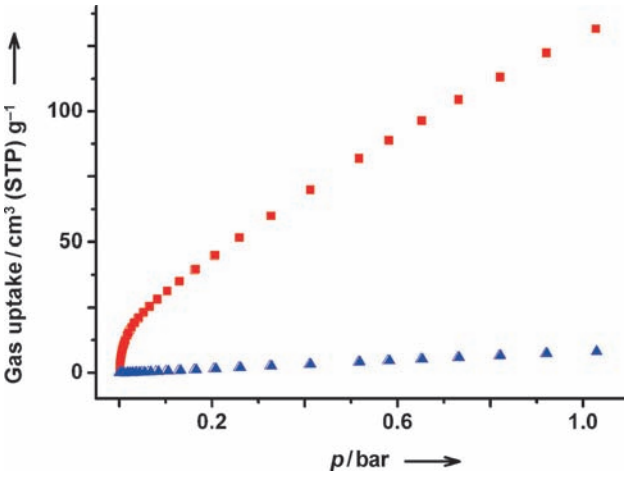

Figure 2. CO_2 and N_2 sorption isotherms of Cu-TDPAT at 298 K (adsorption: filled; desorption: open; CO_2: red squares; N_2: blue triangles).

high CO_2 binding affinity can be attributed to the fact that **1** is the only member that also carries a high density of LBSs and that has the smallest cages.

To further understand the nature of interactions between CO_2 and the framework, we performed room-temperature IR absorption measurements. Three distinct IR absorption bands of adsorbed CO_2 in **1** are identified, as shown in Figure S21 in the Supporting Information.[21] The appearance of multiple CO_2 IR bands indicates that there are more than one strong adsorbing center. The bands at $\tilde{\nu} = 2335$ and 2342 cm^{-1}, red-shifted by $\tilde{\nu}$ of about -14 and -7 cm^{-1} from the unperturbed value of CO_2 asymmetric stretch ($\tilde{\nu} = 2349$ cm^{-1}), are attributed to CO_2 adsorption sites at the LBS and phenyl rings, respectively.[22] The slightly blue-shifted band at $\tilde{\nu} = 2351$ cm^{-1} ($\tilde{\nu} = \approx +2$ cm^{-1} shift) is attributed to CO_2 interacting through its oxygen with the unsaturated metal centers in a linear adsorption configuration.[23] The lower intensity of the band at $\tilde{\nu} = 2351$ cm^{-1} as compared to that of $\tilde{\nu} = 2335$ cm^{-1} indicates that less CO_2 is present for that specific site, consistent with the fact that **1** has a higher density of LBSs (3.52 nm^3) than that of OMSs (1.76 nm^3). These assignments are consistent with observed changes in the vibrations of **1** upon CO_2 loading (see Figure S21 in the Supporting Information, right panel).

The high Q_{st} values place **1** among a small group of all MOFs having the record high CO_2 binding affinity, including amino-MIL-53 (Al; 38.4 kJ mol^{-1}),[16b] bio-MOF-11 (45 kJ mol^{-1}),[16c] and MOF-74-Mg (47 kJ mol^{-1}).[8a] The value is also close to that of NaX (48.2 kJ mol^{-1}), a zeolite that is used in commercial separation processes based on pressure swing adsorption (PSA).[21]

In addition to its high uptake capacity and strong adsorption enthalpy for CO_2, **1** also shows high adsorption selectivity of CO_2 over N_2 at 298 K. At 1 atm, the separation ratio for CO_2/N_2 calculated based on single-component gas adsorption isotherms is 16 *v*/*v*, higher than those of MOF-74-Mg (12 *v*/*v*)[8a] and ZIF-78 (about 13 *v*/*v*)[4b] under the same conditions. At 0.16 atm (a pressure close to the CO_2 concentration in a power plant flue gas stream), the value is 34 *v*/*v* for **1**, second to the highest value reported for MOF-74-Mg (49 *v*/*v*). To imitate the separation behavior of **1** under a more real-world setting, the CO_2/N_2 selectivity in a binary mixture was calculated employing the ideal adsorbed solution theory (IAST) method[5b,22] with the experimental single-component isotherms fitted by the dual-site Langmuir (DSL) model.[23] At a total pressure of 1 atm and CO_2 concentration of 10% (partial pressure of 0.1 atm), a remarkable selectivity of about 79 is predicted by IAST (see Figure S9 in the Supporting Information).

To evaluate the performance of compound **1** in a real gas mixture, we carried out a series of breakthrough experiments to determine its CO_2 separation capacity from a CO_2/N_2 mixture under kinetic flow conditions (see Figures S11 and S12 in the Supporting Information). The results show that **1** can effectively capture CO_2 from the mixed gas with an uptake of 6.7 wt% before breakthrough, comparable to that of MOF-74-Mg in a similar CO_2/CH_4 breakthrough experiment.[12d] Moreover, compound **1** saturated with CO_2 can be fully regenerated under relatively mild conditions. Successive breakthrough experiments revealed that **1** retains a constant capacity of 5.7 wt% upon repeated regenerations at 80 °C (see the Supporting Information). These values reflect the kinetic aspect of separation, suggesting that **1** is a promising candidate for CO_2 capture and separation from gas mixtures.

The high-pressure gas (CO_2, H_2, CH_4) adsorption of **1** has also been studied. The adsorption data indicate that **1** shows extremely high gas uptake capacity [CO_2 (excess): 310 *v*/*v*, 298 K, 48 bar; H_2 (total): 6.77 wt%, 52.8 g L^{-1}, 77 K, 67 bar; CH_4 (total): 181 *v*/*v*, 298 K, 35 bar]. These values place it among the leading MOF materials to date for CO_2, H_2, and CH_4 storage. Detailed information is provided in the Supporting Information (see Figure S13–20 in the Supporting Information).

In summary, the smallest member of *rht*-type MOFs, Cu-TDPAT built on a hexacarboxylate ligand with imino triazine backbone, shows a greatly enhanced CO_2 binding affinity compared with all other isoreticular *rht*-MOFs and remarkable selectivity of CO_2 over N_2 under conditions that mimic flue gas mixtures. The high adsorption affinity and capacity are attributed to the dual functionalization of the framework by concurrent incorporation of high density of open metal sites and Lewis basic sites. In addition, narrower pores in Cu-TDPAT are likely to be the other contributing factor leading to the stronger CO_2–framework interactions with respect to other similar *rht*-type MOFs. Coupled with its exceptionally high water and thermal stability, Cu-TDPAT may have real promise for adsorption-based small gas separations, in particular CO_2 capture from power plant flue gases.

Experimental Section

The crystal data for Cu-TDPAT are: $C_{27}H_{18}Cu_3N_6O_{15}$, $M = 857.09$, tetragonal, space group $I4/m$, $a = 26.860(4)$, $b = 26.860(4)$, $c = 37.753(8)$, $V = 27238(8)$, $Z = 16$, $F_{000} = 6864$, $R_1 = 0.0621$, and $wR_2 = 0.1513$. Full experimental details are given in the Supporting Information.

CCDC 831219 contains the supplementary crystallographic data. These data can be obtained free of charge from The Cambridge

Crystallographic Data Centre via www.ccdc.cam.ac.uk/data_request/cif.

Received: August 23, 2011
Revised: December 5, 2011
Published online: December 23, 2011

Keywords: carbon dioxide capture · gas separation · Lewis basic sites · metal–organic frameworks · open metal sites

[1] a) J. Lee, O. K. Farha, J. Roberts, K. A. Scheidt, S. T. Nguyen, J. T. Hupp, *Chem. Soc. Rev.* **2009**, *38*, 1450 – 1459; b) J.-R. Li, R. J. Kuppler, H.-C. Zhou, *Chem. Soc. Rev.* **2009**, *38*, 1477 – 1504; c) S. Ma, H.-C. Zhou, *Chem. Commun.* **2010**, *46*, 44 – 53; d) D. M. D'Alessandro, B. Smit, J. R. Long, *Angew. Chem.* **2010**, *122*, 6194 – 6219; *Angew. Chem. Int. Ed.* **2010**, *49*, 6058 – 6082; e) A. Phan, C. J. Doonan, F. J. Uribe-Romo, C. B. Knobler, M. O'Keeffe, O. M. Yaghi, *Acc. Chem. Res.* **2009**, *43*, 58 – 67; f) L. Ma, C. Abney, W. Lin, *Chem. Soc. Rev.* **2009**, *38*, 1248 – 1256.

[2] H. Furukawa, N. Ko, Y. B. Go, N. Aratani, S. B. Choi, E. Choi, A. O. Yazaydin, R. Q. Snurr, M. O'Keeffe, J. Kim, O. M. Yaghi, *Science* **2010**, *329*, 424 – 428.

[3] X. Lin, J. Jia, X. Zhao, K. M. Thomas, A. J. Blake, G. S. Walker, N. R. Champness, P. Hubberstey, M. Schröder, *Angew. Chem.* **2006**, *118*, 7518 – 7524; *Angew. Chem. Int. Ed.* **2006**, *45*, 7358 – 7364.

[4] a) Y. Goto, H. Sato, S. Shinkai, K. Sada, *J. Am. Chem. Soc.* **2008**, *130*, 14354 – 14355; b) R. Banerjee, H. Furukawa, D. Britt, C. Knobler, M. O'Keeffe, O. M. Yaghi, *J. Am. Chem. Soc.* **2009**, *131*, 3875 – 3877.

[5] a) L. J. Murray, M. Dinca, J. R. Long, *Chem. Soc. Rev.* **2009**, *38*, 1294 – 1314; b) Y.-S. Bae, O. K. Farha, A. M. Spokoyny, C. A. Mirkin, J. T. Hupp, R. Q. Snurr, *Chem. Commun.* **2008**, 4135 – 4137.

[6] Y.-S. Bae, O. K. Farha, J. T. Hupp, R. Q. Snurr, *J. Mater. Chem.* **2009**, *19*, 2131 – 2134.

[7] R. T. Yang, *Adsorbents*: *Fundamentals and Applications*, Wiley, Hoboken, **2003**.

[8] a) S. R. Caskey, A. G. Wong-Foy, A. J. Matzger, *J. Am. Chem. Soc.* **2008**, *130*, 10870 – 10871; b) H.-S. Choi, M. P. Suh, *Angew. Chem.* **2009**, *121*, 6997 – 7001; *Angew. Chem. Int. Ed.* **2009**, *48*, 6865 – 6869; c) H. Wu, R. S. Reali, D. A. Smith, M. C. Trachtenberg, J. Li, *Chem. Eur. J.* **2010**, *16*, 13951 – 13954.

[9] D. Sun, S. Ma, Y. Ke, D. J. Collins, H.-C. Zhou, *J. Am. Chem. Soc.* **2006**, *128*, 3896 – 3897.

[10] a) W. Morris, B. Leung, H. Furukawa, O. K. Yaghi, N. He, H. Hayashi, Y. Houndonougbo, M. Asta, B. B. Laird, O. M. Yaghi, *J. Am. Chem. Soc.* **2010**, *132*, 11006 – 11008; b) Y. Zhao, H. Wu, T. J. Emge, Q. Gong, N. Nijem, Y. J. Chabal, L. Kong, D. C. Langreth, H. Liu, H. Zeng, J. Li, *Chem. Eur. J.* **2011**, *17*, 5101 – 5109.

[11] a) S. S. Han, W.-Q. Deng, W. A. Goddard, *Angew. Chem.* **2007**, *119*, 6405 – 6408; *Angew. Chem. Int. Ed.* **2007**, *46*, 6289 – 6292; b) F. Debatin, A. Thomas, A. Kelling, N. Hedin, Z. Bacsik, I. Senkovska, S. Kaskel, M. Junginger, H. Müller, U. Schilde, C. Jäger, A. Friedrich, H.-J. Holdt, *Angew. Chem.* **2010**, *122*, 1280 – 1284; *Angew. Chem. Int. Ed.* **2010**, *49*, 1258 – 1262; c) R. Banerjee, A. Phan, B. Wang, C. Knobler, H. Furukawa, M. O'Keeffe, O. M. Yaghi, *Science* **2008**, *319*, 939 – 943; d) J. An, N. L. Rosi, *J. Am. Chem. Soc.* **2010**, *132*, 5578 – 5579; e) S.-M. Zhang, Z. Chang, T.-L. Hu, X.-H. Bu, *Inorg. Chem.* **2010**, *49*, 11581 – 11586; f) S. S. Han, J. L. Mendoza-Cortes, W. A. Goddard III, *Chem. Soc. Rev.* **2009**, *38*, 1460 – 1476.

[12] a) B. Chen, N. W. Ockwig, A. R. Millward, D. S. Contreras, O. M. Yaghi, *Angew. Chem.* **2005**, *117*, 4823 – 4827; *Angew. Chem. Int. Ed.* **2005**, *44*, 4745 – 4749; b) X.-S. Wang, S. Ma, P. M. Forster, D. Yuan, J. Eckert, J. J. López, B. J. Murphy, J. B. Parise, H.-C. Zhou, *Angew. Chem.* **2008**, *120*, 7373 – 7376; *Angew. Chem. Int. Ed.* **2008**, *47*, 7263 – 7266; c) K. Gedrich, I. Senkovska, N. Klein, U. Stoeck, A. Henschel, M. R. Lohe, I. A. Baburin, U. Mueller, S. Kaskel, *Angew. Chem.* **2010**, *122*, 8667 – 8670; *Angew. Chem. Int. Ed.* **2010**, *49*, 8489 – 8492; d) D. Britt, H. Furukawa, B. Wang, T. G. Glover, O. M. Yaghi, *Proc. Natl. Acad. Sci. USA* **2009**, *106*, 20637 – 20640; e) A. R. Millward, O. M. Yaghi, *J. Am. Chem. Soc.* **2005**, *127*, 17998 – 17999; f) D. Yuan, D. Zhao, D. Sun, H.-C. Zhou, *Angew. Chem.* **2010**, *122*, 5485 – 5489; *Angew. Chem. Int. Ed.* **2010**, *49*, 5357 – 5361; g) B. Zheng, J. Bai, J. Duan, L. Wojtas, M. J. Zaworotko, *J. Am. Chem. Soc.* **2010**, *133*, 748 – 751.

[13] a) F. Nouar, J. F. Eubank, T. Bousquet, L. Wojtas, M. J. Zaworotko, M. Eddaoudi, *J. Am. Chem. Soc.* **2008**, *130*, 1833 – 1835; b) A. J. Cairns, J. A. Perman, L. Wojtas, V. C. Kravtsov, M. H. Alkordi, M. Eddaoudi, M. J. Zaworotko, *J. Am. Chem. Soc.* **2008**, *130*, 1560 – 1561.

[14] a) D. Zhao, D. Yuan, D. Sun, H.-C. Zhou, *J. Am. Chem. Soc.* **2009**, *131*, 9186 – 9188; b) Y. Zou, M. Park, S. Hong, M. S. Lah, *Chem. Commun.* **2008**, 2340 – 2342; c) S. Hong, M. Oh, M. Park, J. W. Yoon, J.-S. Chang, M. S. Lah, *Chem. Commun.* **2009**, 5397 – 5399; d) Y. Yan, I. Telepeni, S. Yang, X. Lin, W. Kockelmann, A. Dailly, A. J. Blake, W. Lewis, G. S. Walker, D. R. Allan, S. A. Barnett, N. R. Champness, M. Schröder, *J. Am. Chem. Soc.* **2010**, *132*, 4092 – 4094; e) Y. Yan, X. Lin, S. Yang, A. J. Blake, A. Dailly, N. R. Champness, P. Hubberstey, M. Schroder, *Chem. Commun.* **2009**, 1025 – 1027.

[15] O. K. Farha, A. Özgür Yazaydın, I. Eryazici, C. D. Malliakas, B. G. Hauser, M. G. Kanatzidis, S. T. Nguyen, R. Q. Snurr, J. T. Hupp, *Nat. Chem.* **2010**, *2*, 944 – 948.

[16] a) R. Vaidhyanathan, S. S. Iremonger, K. W. Dawson, G. K. H. Shimizu, *Chem. Commun.* **2009**, 5230 – 5232; b) S. Couck, J. F. M. Denayer, G. V. Baron, T. Rémy, J. Gascon, F. Kapteijn, *J. Am. Chem. Soc.* **2009**, *131*, 6326 – 6327; c) J. An, S. J. Geib, N. L. Rosi, *J. Am. Chem. Soc.* **2009**, *131*, 38 – 39; d) J.-B. Lin, J.-P. Zhang, X.-M. Chen, *J. Am. Chem. Soc.* **2010**, *132*, 6654 – 6656.

[17] L. Spek, *PLATON*: *A Multipurpose Crystallographic Tool*, Utrecht University, Utrecht, The Netherlands, **2001**.

[18] a) K. S. Walton, R. Q. Snurr, *J. Am. Chem. Soc.* **2007**, *129*, 8552 – 8556; b) Y.-S. Bae, A. O. z. r. Yazaydın, R. Q. Snurr, *Langmuir* **2010**, *26*, 5475 – 5483; c) J. Rouquerol, P. Llewellyn, F. Rouquerol, *Stud. Surf. Sci. Catal.* **2007**, *160*, 49 – 56.

[19] R. S. Franchi, P. J. E. Harlick, A. Sayari, *Ind. Eng. Chem. Res.* **2005**, *44*, 8007 – 8013.

[20] a) A. Ansón, J. Jagiello, J. B. Parra, M. L. Sanjuán, A. M. Benito, W. K. Maser, M. T. Martínez, *J. Phys. Chem. B* **2004**, *108*, 15820 – 15826; b) L. Czepirski, J. JagieLlo, *Chem. Eng. Sci.* **1989**, *44*, 797 – 801; c) J. Jagiełło, T. J. Bandosz, J. A. Schwarz, *Langmuir* **1996**, *12*, 2837 – 2842.

[21] D. Shen, M. Bülow, F. Siperstein, M. Engelhard, A. L. Myers, *Adsorption* **2000**, *6*, 275 – 286.

[22] a) Y.-S. Bae, K. L. Mulfort, H. Frost, P. Ryan, S. Punnathanam, L. J. Broadbelt, J. T. Hupp, R. Q. Snurr, *Langmuir* **2008**, *24*, 8592 – 8598; b) M. Heuchel, R. Q. Snurr, E. Buss, *Langmuir* **1997**, *13*, 6795 – 6804; c) A. L. Myers, J. M. Prausnitz, *AICHE J.* **1965**, *11*, 121 – 127.

[23] a) S. Keskin, J. Liu, J. K. Johnson, D. S. Sholl, *Langmuir* **2008**, *24*, 8254 – 8261; b) S. Keskin, J. Liu, R. B. Rankin, J. K. Johnson, D. S. Sholl, *Ind. Eng. Chem. Res.* **2009**, *48*, 2355 – 2371.

